European Radiology (2019) 29:1527–1537
https://doi.org/10.1007/s00330-018-5665-y

PAEDIATRIC

Proper timing for the evaluation of neonatal brain white matter development: a diffusion tensor imaging study

Chao Jin[1] · Yanyan Li[1] · Xianjun Li[1] · Miaomiao Wang[1] · Congcong Liu[1] · Jie Gao[1] · Qinli Sun[1] · Deqiang Qiu[2] · Lingxia Zeng[3] · Xihui Zhou[4] · Gailian Li[4] · Jinni Zhang[5] · Jie Zheng[6] · Jian Yang[1]

Received: 27 April 2018 / Revised: 27 June 2018 / Accepted: 13 July 2018 / Published online: 27 August 2018

Abstract

Objective We aimed to determine the timing for assessing birth status of the developing brain (i.e. brain maturity at birth) by exploring the postnatal age-related changes in neonatal brain white matter (WM).

Methods The institutional review board approved this study and all informed parental consents were obtained. 133 neonates (gestational age, 30–42 weeks) without abnormalities on MRI were studied with regard to WM development by diffusion tensor imaging-derived fractional anisotropy (FA). Tract-based spatial statistics (TBSS), locally-weighted scatterplot smoothing (LOESS) and piecewise linear-fitting were used to investigate the relationship between FA and postnatal age. FA along corticospinal tract (CST), optic radiation (OR), auditory radiation (AR) and thalamus-primary somatosensory cortex (thal-PSC) were extracted by automated fibre-tract quantification; their differences and associations with neonatal neurobehavioural scores at various postnatal age ranges were analysed by Wilcoxon's rank-sum test and Pearson's correlation.

Results Using TBSS, postnatal age (days 1–28) positively correlated with FA in multiple WMs, including CST, OR, AR and thal-PSC ($p<0.05$). On the other hand, when narrowing the postnatal age window to days 1–14, no significant correlation was found, suggesting a biphasic WM development. LOESS and piecewise linear-fitting indicated that FA increased mildly before day 14 and its growth accelerated thereafter. Both FA and correlations with neurobehavioural scores in postnatal age range 2 (days 15–28) were significantly higher than in range 1 (days 1–14) (FA comparison: $p<0.05$; maximal correlation-coefficient: 0.693 vs. 0.169).

Conclusion Brain WM development during the neonatal stage includes two phases, i.e. a close-to-birth period within the first 14 days and a following accelerated maturation period. Therefore, evaluations of birth status should preferably be performed during the first period.

Key Points

- *Brain white matter development within the first two postnatal weeks resembles a close-to-birth maturation.*
- *Brain white matter development in the audio-visual, sensorimotor regions accelerates after two postnatal weeks.*
- *Postnatal age-related effects should be considered in comparing preterm and term neonates.*

Keywords Newborn · White matter · Child development · Diffusion tensor imaging

Chao Jin and Yanyan Li contributed equally to this study.

Electronic supplementary material The online version of this article (https://doi.org/10.1007/s00330-018-5665-y) contains supplementary material, which is available to authorized users.

✉ Jian Yang
yj1118@mail.xjtu.edu.cn

[1] Department of Radiology, the First Affiliated Hospital of Xi'an Jiaotong University, Xi'an 710061, People's Republic of China

[2] Department of Radiology and Imaging Sciences, Emory University, Atlanta, GA 30322, USA

[3] Department of Epidemiology and Health Statistics, School of Public Health, Xi'an Jiaotong University Health Science Center, Xi'an 710054, People's Republic of China

[4] Department of Neonatology, the First Affiliated Hospital of Xi'an Jiaotong University, Xi'an 710061, People's Republic of China

[5] Department of Pediatric, the First Affiliated Hospital of Xi'an Jiaotong University, Xi'an 710061, People's Republic of China

[6] Clinical Research Center, the First Affiliated Hospital of Xi'an Jiaotong University, Xi'an 710061, People's Republic of China

Abbreviations

AR	Auditory radiation
CST	Corticospinal tract
DTI	Diffusion tensor imaging
FA	Fractional anisotropy
GA	Gestational age
LOESS	Locally-weighted scatterplot smoothing
MR imaging	Magnetic resonance imaging
OR	Optic radiation
TBSS	Tract-based spatial statistics
thal-PSC	Thalamus-primary somatosensory cortex
WM	White matter

Introduction

Neonatal assessment at birth is a clinically indispensable procedure for determining developmental status, and thereby guide the appropriate care and timely intervention [1, 2]. In addition, birth status assessment of brain development would facilitate the more in-depth identification of neurodevelopmental maturity at birth [3–5]. However, immediate evaluation following birth is practically unachievable, particularly for extremely preterm neonates who have remarkably unstable physiological signs and vulnerability [6, 7]. Clinical protocols used to assess neonatal brain development, e.g. neuroimaging and neurobehavioural assessments, are commonly performed when neonates' physiological status stabilizes after a few days [8–10]. It is unclear how well such assessments reflect developmental stage or abnormalities of the brain at birth, as there is evidence that the extra-uterine environment can affect the brain development trajectory together with genetic and epigenetic factors [11]. For example, animal studies have found accelerated brain white matter (WM) myelination induced by elevated light stimulation [12, 13]. Such factors confound the precise evaluation of birth status. Furthermore, abnormalities of preterm brain development identified at a term-equivalent age [5, 11] may also be confounded. Therefore, how to correctly time birth status assessment of neonatal brain development becomes a concern. It is worth noting that Broekman et al have observed no significant relationship between whole-brain WM microstructural metrics and postnatal age at magnetic resonance (MR) imaging (days from birth to MR imaging visit; range, 5–17 days) in term-born neonates [14]. This may suggest the possible existence of a period close to the time of birth during the neonatal stage wherein these assessments can be performed. Detailing the postnatal age-related changes in neonatal brain WM development may thus provide us with solutions to determining the timing for evaluation of birth status. To address this issue, diffusion tensor imaging (DTI)-derived fractional anisotropy (FA), which allows *in vivo* quantification of brain WM microstructural changes [3, 15–17], was used to explore postnatal age-related changes. Neonatal neurobehavioural assessment reflecting the developmental status of functional abilities was used to validate postnatally dynamic changes in brain WM.

Materials and methods

The institutional review board approved this retrospective study and informed parental consent was obtained for all study participants.

Participants

Between December 2010 and September 2017, 664 neonates who underwent MR imaging examinations were retrospectively recruited from the department of neonatology at the first author's affiliation. 251 neonates (gestational age [GA] range, 30–42 weeks) who met the following inclusion criteria were enrolled: successful completion of MR imaging examination; postnatal age range of 1–28 days at MR imaging; birth size appropriate for GA; and normal neurodevelopment outcome at age of 6–30 months (assessed by the Bayley Scales of Infant Development, second edition).

Neonates with abnormalities on MR images and/or neonatal diseases, such as cerebral infection, congenital malformation, metabolic disorders, punctate white matter lesions, diffuse excessive high signal intensity, periventricular leukomalacia, cortical infarction and intracranial haemorrhage (diagnosed by supplementary susceptibility weighted imaging, if necessary) were excluded. Neonates with MR imaging artefacts affecting data analysis were excluded. Furthermore, neonates of mothers with gestational diabetes, hypertension, hypoglycaemia and a history of alcohol during pregnancy were also excluded.

MR imaging data acquisition

The MR imaging data were acquired using a 3.0-T scanner (Signa HDxt, GE Healthcare, Milwaukee, WI, USA) with an 8-channel head coil. The brain MR imaging was carried out on the neonates during natural sleep (i.e. adopting sleep deprivation and/or feeding protocols); for neonates who could not remain still, sedation using an oral administration of 10% chloral hydrate (dose: 25–50 mg/kg) was used to reduce the head motion during the examination. Given the potential risks of chloral hydrate, patient selection, monitoring and management were strictly performed according to guidelines [18]; adverse drug reactions within 24 h following sedation were also followed up. Earplugs and sponge-mats were used for

hearing protection. Heart rate, transcutaneous oxygen saturation and respiration rate were synchronously monitored. The MR imaging protocols included three-dimensional T1-weighted imaging, T2-weighted imaging and DTI (Table 1).

The MR images were independently reviewed by two experienced radiologists with 5 and 7 years, respectively, of paediatric MRI experiences in consensus.

Neonatal neurobehavioural development assessment

Using neonatal behavioural neurological assessment (Chinese) [19] and Dubowitz neurological assessment as references [20], two neurobehavioural categories, i.e., behaviour (six items) and active tone (four items), were used to assess neonatal functional abilities within 5 days before or after MR imaging. Each item was scored on a three-point scale (0, 1 and 2). Two neonatologists with 25 and 30 years of experience, respectively, independently conducted the assessments in consensus.

DTI processing and statistical analysis

DTI processing and data harmonisation DTI data were processed using the FMRIB software library (www.fmrib.ox.ac.uk/fsl). Brain Extraction Tool was used to extract the brain and FMRIB's Diffusion Toolbox was used to correct the eddy currents and head motion-induced distortions, to estimate the diffusion tensor and to calculate the FA mappings. Combat harmonisation [21] for FA data between two DTI protocols was performed because of their significant differences ($p<0.001$; see details in Online Supplemental Material).

Tract-based spatial statistics (TBSS) TBSS was performed by an optimised pipeline for neonates [22]. All of the FA images were normalised to the Johns Hopkins neonatal template. The aligned FA image of each subject was projected onto the mean FA skeleton (threshold=0.15). General linear model (GLM) was used to separately assess the relationships between FA and postnatal age at MR imaging (day) for preterm (n=57), term (n=76) and all neonates (n=133). Relationships between FA and background characteristics (maternal age, education level and family socioeconomic status) were first evaluated to determine whether these characteristics should be considered as covariates in addition to the set covariates, i.e. GA, adjusted anthropometric indicators (birth weight, head circumference and crown-heel length), and sex. Birth anthropometric indicators were adjusted for GA because of their confirmed strong relationships ($p<0.05$). GLM was performed using GA as a covariate for the limited number of preterm and term neonates. The number of permutations was set to 5,000. The results of all tests were considered significant when $p<0.05$ after family-wise error rate correction with threshold-free cluster enhancement.

Scatterplots with fitting between FA and postnatal age Considering the complexity of brain development [23], a locally weighted scatterplot smoothing model (LOESS), which requires no assumptions regarding linear or non-linear patterns within the data [23–25], was used to study the postnatal age-related changes in mean adjusted FA. Four visual, auditory and sensorimotor WMs extracted using the Johns Hopkins atlas were selected as regions of interest (ROIs). These regions were optic radiation (OR), auditory radiation (AR), corticospinal tract (CST) and thalamus-primary somatosensory cortex (thal-PSC). The inflection point of the LOESS fitted curve was determined as the second derivation closest to zero. Furthermore, piecewise linear fitting was employed to explore the respective relationships of adjusted FA with postnatal age at various postnatal age ranges that were divided by the inflection points. FA was adjusted using multiple linear regression with GA, adjusted anthropometric indicators and sex as covariates.

Table 1 Magnetic resonance imaging protocols and scanning parameters

Scanning parameters	3D-T1WI	T2WI	DTI protocol1	DTI protocol2
Repetition time (ms)	10	4,200	5,500	11,000
Echo time (ms)	4.6	120	95	69.5
Field of view (cm)	24	18	18	18
Matrix acquisition	240×240	256×256	128×128	128×128
Slice thickness (mm)	1	4	4	2.5
Number of excitations	1	1.5	1	1
Direction number	--	--	35	30
b value (s/mm^2)	--	--	1000	600

3D-T1WI three-dimensional fast spoiled gradient echo T1-weighted imaging, *T2WI* transverse fast spin-echo T2-weighted imaging, *DTI* diffusion tensor imaging

Comparison of FA along the fibre tracts at various postnatal age ranges DTI-based 3D automated fibre-tract quantification (AFQ) was performed to study differences in FA at various postnatal age ranges [26]. The aligned FA images obtained following the TBSS procedure were projected onto the Johns Hopkins probabilistic maps of fibre tracts [27]. FA along the bilateral OR, AR, CST and thal-PSC were extracted. Mean FA at the cross-section perpendicular to the fibre tract was calculated. The fibre tract was divided into 100 segments, and the cross-section was each segment's vertical section (denoted as sections 0–100). FA was first adjusted using the regression model described above. The Wilcoxon rank sum test was then used to compare differences in adjusted FA at various postnatal age ranges.

Correlations between FA and neurobehavioural scores at various postnatal age ranges Pearson correlation analyses between neurobehavioural scores and mean FA within the bilateral CST, OR, AR and thal-PSC were performed to evaluate the differences in the relationship between FA and neurological development at various postnatal age ranges.

All regression analyses were performed using SPSS software (SPSS version 17.0; SPSS, Inc., Chicago, IL, USA). The scatterplots, calculation of the inflection point of LOESS curves, piecewise linear fitting and correlation analyses were performed using MATLAB software (MATLAB version R2012b; The Mathworks, Inc., Natick, MA, USA). *p*-values <0.05 were considered statistically significant.

Results

Participant demographics

Of the 251 neonates, 133 (GA range, 30–42 weeks) without abnormalities on MRI within 28 days after birth were included (Fig. 1, Table 2).

Relationship between postnatal age and brain WM FA

TBSS results found that birth indicators, i.e. GA and birth weight, showed significant correlations with FA (see details in Online Supplemental Material), while no correlation was found in background characteristics (i.e. maternal age, education level and family socioeconomic status).

For preterm neonates, postnatal age (days 1–28) positively correlated with FA in regional WM, e.g. CST ($p<0.05$, corrected; Fig. 2a), while for term neonates, significant correlations were found in more WM regions, e.g. CST and OR ($p<0.05$, corrected; Fig. 2b). No correlation was found in postnatal ages 1–14 days in either the preterm or the term group.

After controlling for birth indicators and sex, postnatal age (days 1–28) of all neonates had a significant correlation with FA in regional WM, such as the corpus callosum, OR, AR, CST and thal-PSC ($p<0.05$, corrected; Fig. 2c). However, no correlation was found in postnatal ages 1–14 days.

Scatterplots of postnatal age versus brain WM FA

In all neonates, the LOESS fitted curve for CST indicated that an inflection point (day 14, second derivation = -8.04×10^{-6}) divided the postnatal age timeline (days 1–28) into two phases. Similarly, three respective inflection points were also observed for OR (day 13, second derivation = -7.25×10^{-6}), AR (day 12, second derivation = -8.04×10^{-6}) and thal-PSC (day 14, second derivation = -6.13×10^{-6}). These suggested that a time point near day 14 may be seen as an inflection point during the neonatal stage. Piecewise linear fitting results indicated that adjusted FA only slightly varied before this point, while it significantly increased thereafter (Slops at two phases: CST, 0.003 vs. 0.010; OR, 0.003 vs. 0.007; AR, 0.002 vs. 0.009; thal-PSC, 0.002 vs. 0.007) (Fig. 3a).

The biphasic changes of adjusted FA were also observed in preterm and term neonates (Fig. 3b and c; see details in Online Supplemental Material).

Comparisons of FA along fibre tracts between postnatal age range 1 (days 1–14) and range 2 (days 15–28)

The LOESS results suggested that a time point near 14 days divided the postnatal age timeline (days 1–28) into two phases. Therefore, comparisons of FA along the selected WM tracts were performed between postnatal age range 1 (days 1–14, n=96) and range 2 (days 15–28, n=37).

In the CST, the adjusted FA in range 2 was higher than that in range 1 in the initial, middle and terminal segments (left CST, sections 0–24 and 34–81; right CST, sections 0–86; $p<0.05$) (Fig. 4a). In the OR, higher adjusted FA was observed in age range 2 than in range 1 in the left initial and terminal segments (sections 0–29 and 57–91; $p<0.05$) and the right initial, middle and partial terminal segments (sections 0–76; $p<0.05$) (Fig. 4b). In the AR, we found higher adjusted FA in range 2 than in range 1 mainly in the initial and middle segments (left AR, sections 0–69; right AR, sections 0–71; $p<0.05$) (Fig. 4c). Along the thal-PSC, higher adjusted FA was found in range 2 in the initial and middle segments than in range 1 (left thal-PSC, sections 0–72; right thal-PSC, sections 0–69; $p<0.05$) (Fig. 4d).

The higher adjusted FA in range 2 than those in range 1 were also observed in preterm (mainly located at the initial segments)

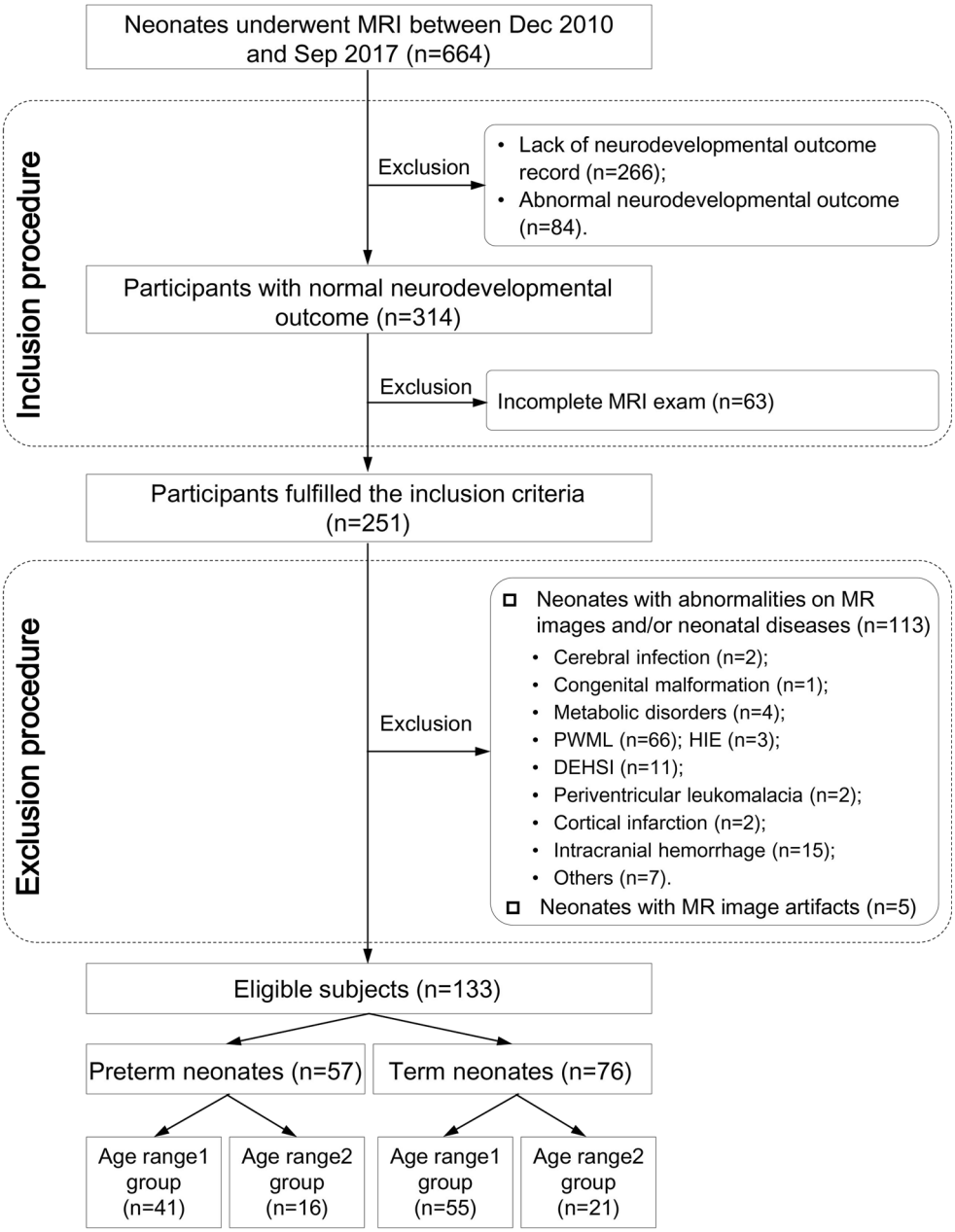

Fig. 1 Flow chart for determining the study subjects based on the inclusion and exclusion criteria. Age range 1 and range 2 denotes postnatal age range 1 (days 1–14) and range 2 (days 15–28), respectively. *PWML* punctate white matter lesion, *HIE* hypoxic ischaemic encephalopathy; *DEHSI* diffuse excessive high signal intensity

and term neonates (mainly located at the initial and middle segments) (see details in Online Supplemental Material).

Pearson's correlations of FA with neurobehavioural scores during postnatal age range 1 (days 1–14) and range 2 (days 15–28)

During postnatal range 1 (days 1–14), no significant correlation between neurobehavioural scores (behaviour and active tone) and mean FA in the CST, OR, AR and thal-PSC was found. Specifically, Pearson's correlation coefficients ranged from 0.026 to 0.169. In contrast, in age range 2 (days 15–28), significant correlations with higher Pearson's coefficients of 0.542–0.693 in the CST, OR, AR and thal-PSC were observed (Table 3).

Discussion

To determine the proper timing for birth status assessment, the postnatal age-related changes in WM development were explored. Our results indicate that within approximately 2 weeks after birth, postnatal age presents no significant correlation with WM FA. However, as a whole, significant correlations of FA with postnatal age are observed during postnatal days 1–28. These may reflect the considerable effect of postnatal age

Table 2 Participant demographics

Clinical characteristics	
Preterm/term	57/76
Males/females	82/51
Gestational age (weeks)[a]	37.1 ± 2.9
Birth weight (g)[a]	2,670.0 ± 843.2
Adjusted birth weight (g)[a]	2,670.0 ± 492.1
Head circumference (cm)[a]	32.64 ± 3.17
Adjusted head circumference (cm)[a]	32.64 ± 2.38
Crown-heel length (cm)[a]	47.42 ± 4.31
Adjusted crown-heel length (cm)[a]	47.42 ± 3.19
Postnatal age at MRI (day)[a]	11.5 ± 6.4
5-min Apgar[a]	9.37 ± 0.95
10-min Apgar[a]	9.76 ± 0.54
Neonatal neurobehavioural assessment[b]	
Behaviour	9.45 ± 1.45
Active tone	5.85 ± 1.66
Background characteristics	
Maternal age (y)[a]	28.89 ± 4.06
Mother no high school education	88 (133)
Prenatal smoking exposure	0 (133)
Minority ethnicity	0 (133)
Family socioeconomic status[c]	
Professional/managerial	20 (133)
Technical/skilled	32 (133)
Semiskilled/unskilled/unemployed	81 (133)

Neonates with no abnormalities on MRI scanned within 28 days after birth

[a] Data represented as mean ± standard deviation

[b] Of 133 neonates, 101 neonates had the recorded neurobehavioural assessment

[c] Assessed using the Elley-Irving socioeconomic index

on brain development. As suggested by our results, early postnatal WM development may include two phases. The first occurs before the approximately 2-week time point, and the second follows with an accelerated maturation.

Considering the interactions between genetic and epigenetic factors in WM development [28], some typical birth indicators, maternal characteristics and family socioeconomic factors were studied. Our results agreed with previous findings [14]. Specifically, typical birth indicators (e.g. GA and birth weight) had significant correlations with FA, while maternal characteristics and family socioeconomic factors had no correlations. In light of this, we used birth factors as covariates in order to eliminate confounding effects on WM maturity.

Correlations of FA in term neonates with GA and postnatal age were studied separately; a significant correlation was found in GA while no significant result in postnatal age during postnatal days 5–17 was found [14]. Similarly, our LOESS and piecewise linear fitting results found that an inflection point near the 14-week time point divided the postnatal timeline into two phases. Before this point, adjusted FA varied slightly, although it increased considerably thereafter. A similar phenomenon was also observed in both preterm and term neonates. All of the above mentioned observations support the definition of a close-to-birth period and further suggest that the first 2 weeks after birth may closely resemble birth conditions, and could thus be referred to as the close-to-birth period.

Using TBSS, postnatal age (days 1–28) of all neonates was found to be statistically related to FA in regional WMs, including CST, OR and AR. Following birth, the neonatal brain is affected by postnatal factors (e.g. light and sound) and undergoes rapid maturation in its visual, auditory and sensorimotor functions [3]. Increasing FA in the corpus callosum and the external capsule may, respectively, indicate the development of commissural and association fibres [29–31]. In addition, significant correlations of FA with postnatal age in preterm neonates were mainly observed in motor-associated WM regions, while term neonates displayed correlations in more WM regions. As GA was controlled, these results may suggest

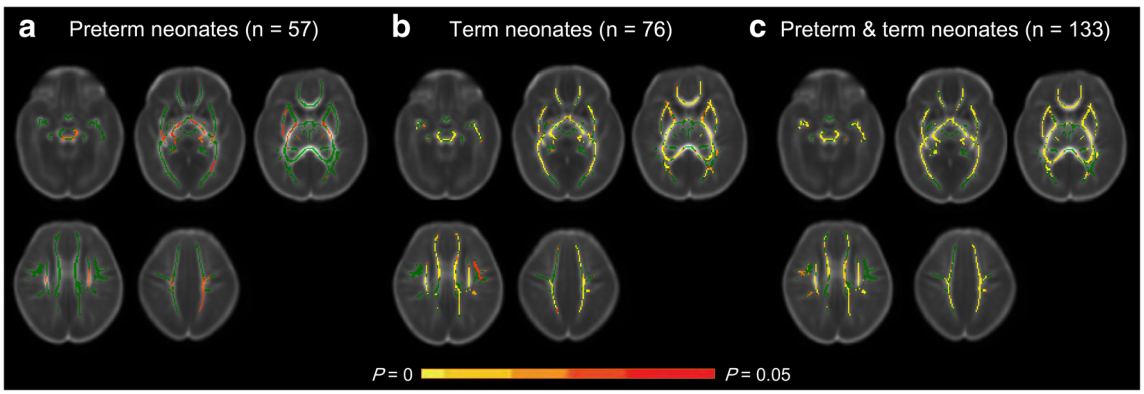

Fig. 2 Correlations between fractional anisotropy (FA) and postnatal age using a general linear model. (**a**) Preterm (n = 57), (**b**) term neonates (n = 76) and (**c**) all neonates (n = 133) within 28 days after birth. Green indicates the fibrous skeleton of brain white matter and the warm-toned colours indicate positive correlations

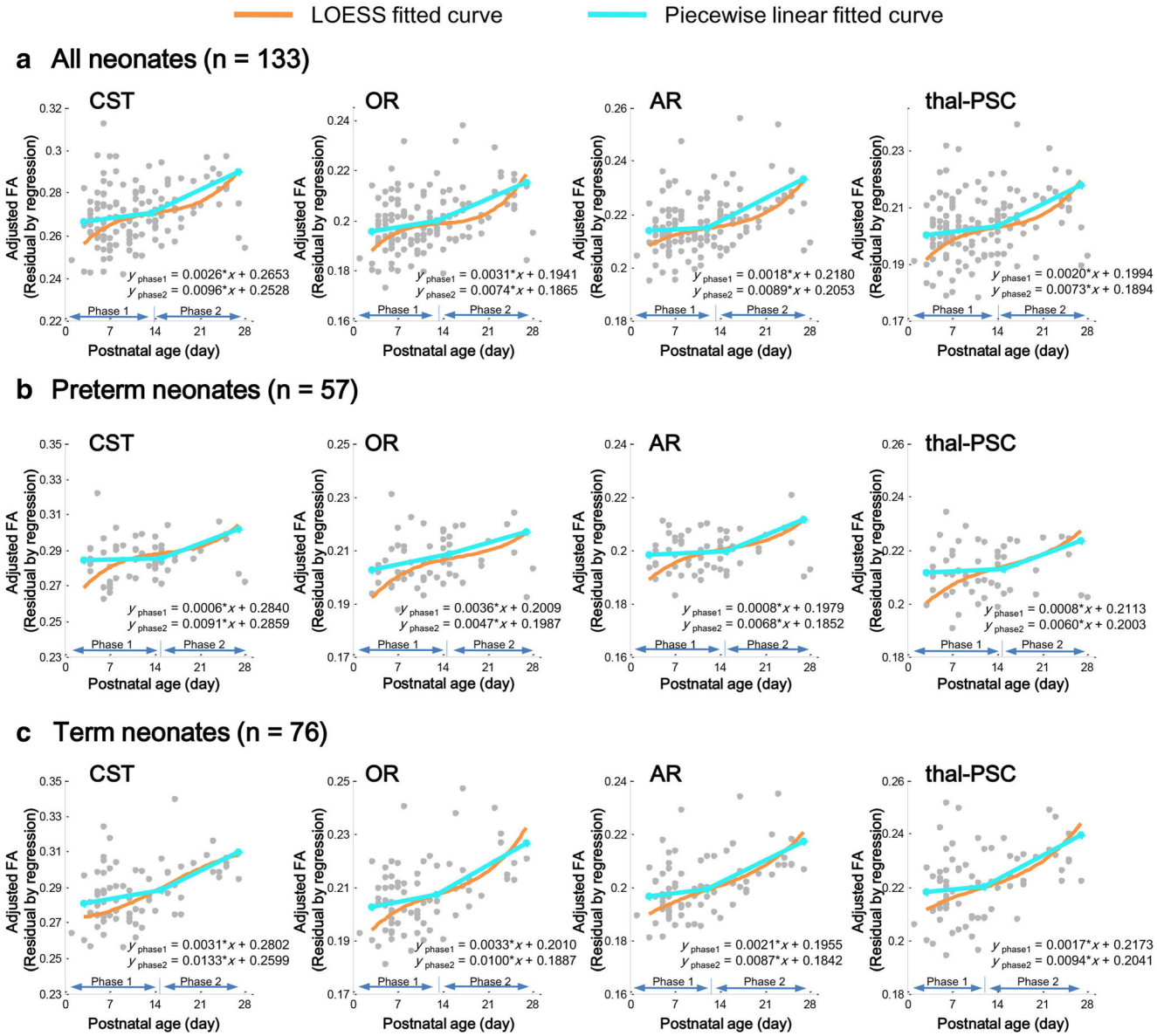

Fig. 3 Scatterplots, locally weighted scatterplot smoothing model (LOESS) and piecewise linear fitted curve between adjusted fractional anisotropy (FA) and postnatal age. (**a**) All neonates (n = 133), (**b**) preterm (n = 57) and (**c**) term neonates (n = 76). Mean FA within the corticospinal tract (CST), optic radiation (OR), auditory radiation (AR) and thalamus-primary somatosensory cortex (thal-PSC) were extracted and studied with postnatal age-related changes. The inflection point divided the postnatal age timeline into two phases; y_{phase1} and y_{phase2} were the respective linear fitted curves at two phases. In all neonates, FA was adjusted using a multiple linear regression with gestational age, adjusted birth weight, adjusted head circumference, adjusted crown-heel length and sex as covariates. Birth weight, head circumference and crown-heel length were first adjusted for gestational age because of their confirmed strong relationships ($p<0.05$). In preterm and term neonates, FA was adjusted by linear regression with gestational age due to the limited sample number

the weaker capacity of postnatal WM maturation in preterm neonates when compared to term neonates.

Our AFQ results indicate that there were higher adjusted FAs in postnatal age range 2 (days 15–28) than in range 1 (days 1–14) in the OR, AR, CST and thal-PSC. This reflects the ongoing myelination in the typical visual, auditory and sensorimotor WM regions. Significant maturation rate differences in the visual, auditory and sensorimotor regions may possibly be correlated with the WM myelination sequence, i.e. central/proximal portions develop earlier than peripheral/distal ones [32–34]. Consequently, significant differences in adjusted FA were predominantly observed at the initial and middle segments of all the WM tracts. It was worth noting that OR presented higher adjusted FA at wider terminal segments in the left tracts than in the right, further suggesting the cerebral lateralisation (left hemispheric dominance) in early brain WM development [35]. This structural asymmetry may underpin the lateralisation of the somatosensory response that is

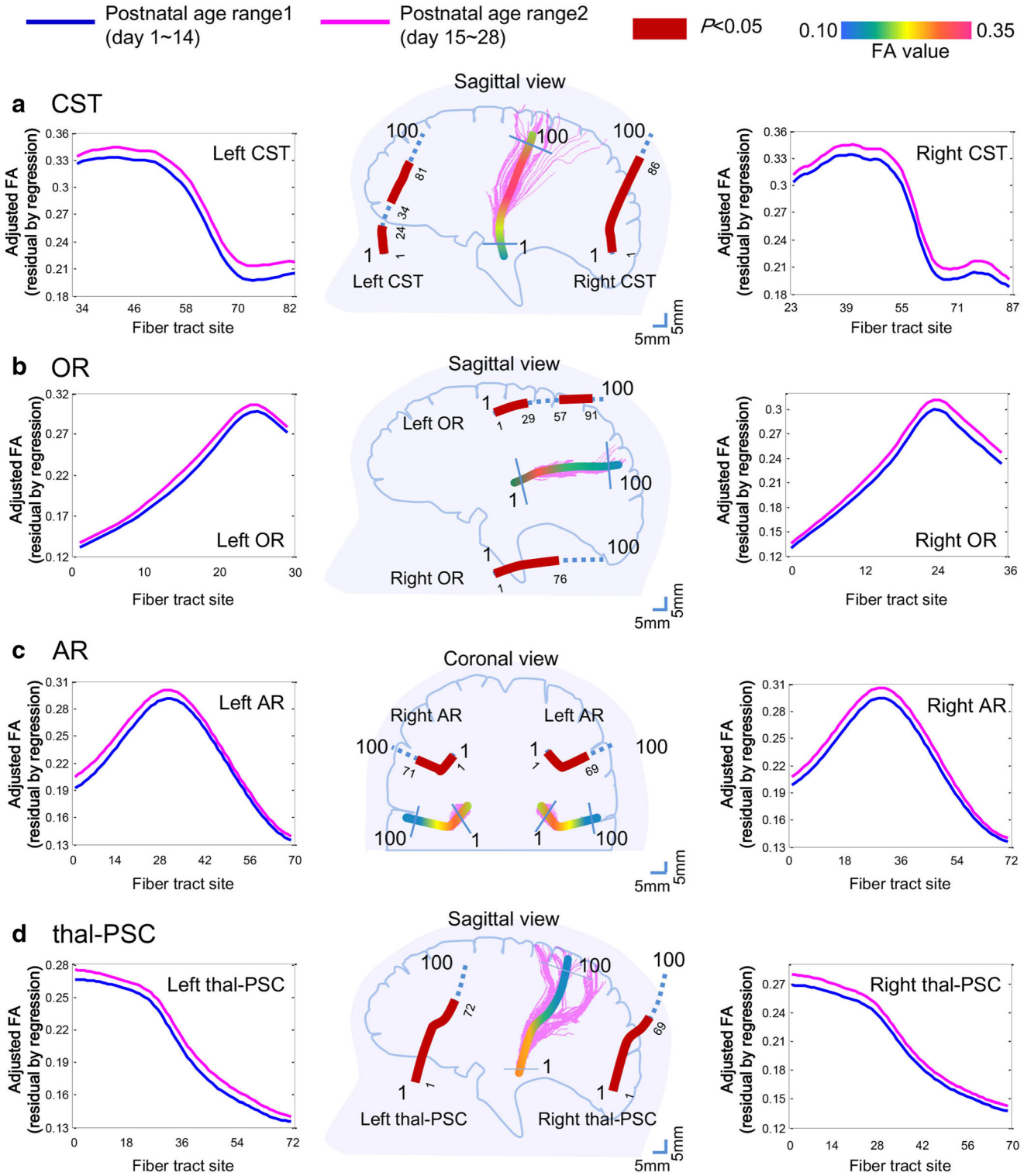

Fig. 4 Comparisons of fractional anisotropy (FA) between postnatal age range 1 (days 1–14) and postnatal age range 2 (days 15–28). (**a**) Corticospinal tract (CST), (**b**) optic radiation (OR), (**c**) auditory radiation (AR) and (**d**) thalamus-primary somatosensory cortex (thal-PSC). The selected fibre tract was divided into 100 segments denoted as sections 0–100. FA was adjusted using multiple linear regression with gestational age, adjusted birth weight, adjusted head circumference, adjusted crown-heel length and sex as covariates. Birth weight, head circumference and crown-heel length were first adjusted for gestational age because of their confirmed strong relationships ($p<0.05$)

detected at birth [36]. In addition, such asymmetry patterns are likely attributable to genetic programs during prenatal stage, as asymmetry of gene expression in the human embryonic cortex has been found at a gestational age of 12 weeks [37].

Table 3 Pearson correlations of brain white matter fractional anisotropy (FA) with neonatal behaviour and active tone scores

	Corticospinal tract (CST)	Optic radiation (OR)	Auditory radiation (AR)	Thalamus-primary somatosensory cortex (thal-PSC)
Postnatal age range 1 (days 1–14)				
Behaviour	0.118	0.101	0.026	0.046
Active tone	0.169	0.082	0.064	0.114
Postnatal age range 2 (days 15–28)				
Behaviour	**0.693**†	**0.542**†	**0.554**†	**0.646**†
Active tone	0.224	0.025	0.066	0.156

Scores of two items, i.e. behaviour and active tone, were used to correlate the FA within the typical white matter regions of interest (ROIs), including corticospinal tract (CST), optic radiation (OR), auditory radiation (AR) and thalamus-primary somatosensory cortex (thal-PSC)

Postnatal age represented the age at MRI, and difference in age between at MRI and at neurobehavioural assessment was -0.8 ± 1.7 days.

†Significance level at $p<0.05$; p-values for CST, OR, AR and thal-PSC were 0.001, 0.014, 0.011 and 0.002, respectively

Pearson's correlations between neurobehavioural scores and FA were higher in postnatal age range 2 (days 15–28) than in range 1 (days 1–14). During the newborn stage, neonatal neurobehavioural development also presented a biphasic growth pattern; however, this was opposite to the WM FA, i.e. slow after the rapid growth (see details in Online Supplemental Material). It may be this that led to the particularly different correlations with behaviour scales during the two periods. These may further suggest accelerated WM maturation during the range 2 period, and would support the presence of the two developmental phases of brain WM. In addition, we found weak correlations between FA and motor-associated scales, especially for CST. This may be due to asynchronous maturation of CST segments. Our findings were consistent with those of previous studies [11].

Our results suggest that postnatal age may be an important factor in investigating the neonatal WM maturation. MRI findings in preterm neonates at term-equivalent age may reflect combined preterm and postnatal factors. Some studies did not take the postnatal factors into account, and imaging results usually directly compared infants born preterm at term-equivalent age to term neonates when characterising developmental differences, e.g. differences in WM maturation [38–40], premature-associated psychomotor delay [5] and regional developmental abnormalities [11]. As suggested by our results, it may be worth considering the postnatal age-related effects during analysis.

Our study had some limitations. The first was the small sample size, especially for neonates aged 15–28 days. Pearson correlations with neurobehavioural scores are thus restricted for preterm and term groups. Larger samples are required to assess changes in WM maturation at various postnatal ages, and to determine a more specified close-to-birth period for each WM tract. Second, although we used Dubowitz neurological assessments as a reference, the efficiency of our neurobehavioural assessments for preterm neonates should be studied further in large-scale surveys. Third, given the complexity of brain development, perinatal factors (e.g. maternal antenatal steroids) potentially affecting brain WM maturation should be considered in future analyses. Additionally, a longitudinal study targeting early brain development is required to better understand the respective roles of natural growth and postnatal factors. Further multicentre longitudinal studies would be of great value in characterising early brain development in the first month of life.

Conclusion

In conclusion, our findings indicate that postnatal age-related changes in neonatal brain WM development present two phases, the first is a close-to-birth period before approximately 14 days after birth, and the second is an accelerated development period. Based on this, clinical protocols used to evaluate the birth status of brain WM maturity may preferably be performed during the first period.

Funding This study has received funding by the National Key Research and Development Program of China (2016YFC0100300), National Natural Science Foundation of China (No. 81171317, 81471631, 81771810 and 51706178), the 2011 New Century Excellent Talent Support Plan of the Ministry of Education, China (NCET-11-0438), China Postdoctoral Science Foundation (No. 2017M613145), Shaanxi Provincial Natural Science Foundation for Youths of China (No. 2017JQ8005), the Clinical Research Award of the First Affiliated Hospital of Xi'an Jiaotong University (No. XJTU1AF-CRF-2015-004) and the Hospital Fund of the First Affiliated Hospital of Xi'an Jiaotong University, China (No. 2016QN-08).

Compliance with ethical standards

Guarantor The scientific guarantor of this publication is Jian Yang, the First Affiliated Hospital of Xi'an Jiaotong University

Conflict of interest The authors of this manuscript declare no relationships with any companies whose products or services may be related to the subject matter of the article.

Statistics and biometry No complex statistical methods were necessary for this paper.

Informed consent Written informed consent was obtained from all subjects (patients) in this study.

Ethical approval Institutional Review Board approval was obtained.

Methodology
- Retrospective
- Observational
- Performed at one institution

References

1. Public Health England (2016) Newborn and infant physical examination: programme handbook. Available via https://www.gov.uk/government/publications/newborn-and-infant-physical-examination-programme-handbook. Accessed 15 Dec 2017
2. Buonocore G, Bracci R, Weindling M (2012) Neonatology. Springer, Milano
3. Dubois J, Dehaene-Lambertz G, Perrin M et al (2008) Asynchrony of the early maturation of white matter bundles in healthy infants: quantitative landmarks revealed noninvasively by diffusion tensor imaging. Hum Brain Mapp 29:14–27
4. Huang H, Zhang J, Wakana S et al (2006) White and gray matter development in human fetal, newborn and pediatric brains. Neuroimage 33:27–38
5. Qiu A, Mori S, Miller MI (2015) Diffusion tensor imaging for understanding brain development in early life. Annu Rev Psychol 66:853–876
6. Stoll BJ, Hansen NI, Bell EF et al (2015) Trends in care practices, morbidity, and mortality of extremely preterm neonates, 1993-2012. JAMA 314:1039–1051
7. Patel RM, Kandefer S, Walsh MC et al (2015) Causes and timing of death in extremely premature infants from 2000 through 2011. N Engl J Med 372:331–340
8. Plaisier A, Govaert P, Lequin MH, Dudink J (2014) Optimal timing of cerebral MRI in preterm infants to predict long-term neurodevelopmental outcome: a systematic review. AJNR Am J Neuroradiol 35:841–847
9. Smyser CD, Kidokoro H, Inder TE (2012) MRI of the brain at term equivalent age in extremely premature neonates - to scan or not to scan? J Paediatr Child Health 48:794–800
10. de Bruïne FT, van den Berg-Huysmans AA, Leijser LM et al (2011) Clinical implications of MR imaging findings in the white matter in very preterm infants: a 2-year follow-up study. Radiology 261:899–906
11. Dubois J, Dehaene-Lambertz G, Kulikova S, Poupon C, Hüppi PS, Hertz-Pannier L (2014) The early development of brain white matter: a review of imaging studies in fetuses, newborns and infants. Neuroscience 276:48–71
12. Tauber H, Waehneldt TV, Neuhoff V (1980) Myelination in rabbit optic nerves is accelerated by artificial eye opening. Neurosci Lett 16:235–238
13. Berman JI, Glass HC, Miller SP et al (2009) Quantitative fiber tracking analysis of the optic radiation correlated with visual performance in premature newborns. AJNR Am J Neuroradiol 30:120–124
14. Broekman BF, Wang C, Li Y et al (2014) Gestational age and neonatal brain microstructure in term born infants: a birth cohort study. PLoS One 9:e115229
15. Partridge SC, Mukherjee P, Henry RG et al (2004) Diffusion tensor imaging: serial quantitation of white matter tract maturity in premature newborns. Neuroimage 22:1302–1314
16. Mukherjee P, McKinstry RC (2006) Diffusion tensor imaging and tractography of human brain development. Neuroimaging Clin N Am 16:19–43
17. Hüppi PS, Dubois J (2006) Diffusion tensor imaging of brain development. Semin Fetal Neonatal Med 11:489–497
18. [No authors listed] (1992) American Academy of Pediatrics Committee on Drugs: Guidelines for monitoring and management of pediatric patients during and after sedation for diagnostic and therapeutic procedures. Pediatrics 89:1110–1115
19. Bao XL, Yu RJ, Li ZS, Zhang BL (1991) Twenty-item behavioral neurological assessment for normal newborns in 12 cities of China. Chin Med J (Eng) 104:742–746
20. Dubowitz LMS, Dubowitz V, Mercuri E (1999) The neurological assessment of the preterm and full-term newborn infant, 2nd edn. Mac Keith Press, London
21. Fortin JP, Parker D, Tunç B et al (2017) Harmonization of multi-site diffusion tensor imaging data. Neuroimage 161:149–170
22. Li X, Gao J, Wang M, Wan M, Yang J (2016) Rapid and reliable tract-based spatial statistics pipeline for diffusion tensor imaging in the neonatal brain: applications to the white matter development and lesions. Magn Reson Imaging 34:1314–1321
23. Fjell AM, Walhovd KB, Westlye LT et al (2010) When does brain aging accelerate? Dangers of quadratic fits in cross-sectional studies. Neuroimage 50:1376–1383
24. Tanaka-Arakawa MM, Matsui M, Tanaka C et al (2015) Developmental changes in the corpus callosum from infancy to early adulthood: a structural magnetic resonance imaging study. PLoS One 10:e0118760
25. Chen H, Zhao B, Cao G et al (2016) Statistical approaches for the study of cognitive and brain aging. Front Aging Neurosci 8:176
26. Yeatman JD, Dougherty RF, Myall NJ, Wandell BA, Feldman HM (2012) Tract profiles of white matter properties: automating fiber-tract quantification. PLoS One 7:e49790
27. Oishi K, Mori S, Donohue PK et al (2011) Multi-contrast human neonatal brain atlas: application to normal neonate development analysis. Neuroimage 56:8–20
28. Gilmore JH, Lin W, Corouge I et al (2007) Early postnatal development of corpus callosum and corticospinal white matter assessed with quantitative tractography. AJNR Am J Neuroradiol 28:1789–1795
29. Kollias S (2012) Insights into the connectivity of the human brain using DTI. NJR 1:78–91
30. Hinkley LBN, Marco EJ, Findlay AM et al (2012) The role of corpus callosum development in functional connectivity and cognitive processing. PLoS One 7:e39804
31. Dean DC 3rd, Planalp EM, Wooten W et al (2017) Mapping white matter microstructure in the one month human brain. Sci Rep 7:9759
32. Nossin-Manor R, Card D, Morris D et al (2013) Quantitative MRI in the very preterm brain: assessing tissue organization and myelination using magnetization transfer, diffusion tensor and T_1 imaging. Neuroimage 64:505–516

33. Rose J, Vassar R, Cahill-Rowley K, Guzman XS, Stevenson DK, Barnea-Goraly N (2014) Brain microstructural development at near-term age in very-low-birth-weight preterm infants: an atlas-based diffusion imaging study. Neuroimage 86:244–256
34. Nelson CA, Luciana M (2008) Handbook of developmental cognitive neuroscience, 2nd edn. MIT Press, Cambridge
35. Gotts SJ, Jo HJ, Wallace GL, Saad ZS, Cox RW, Martin A (2013) Two distinct forms of functional lateralization in the human brain. Proc Natl Acad Sci U S A 110:3435–3444
36. Provenzale JM, Liang L, DeLong D, White LE (2007) Diffusion tensor imaging assessment of brain white matter maturation during the first postnatal year. AJR Am J Roentgenol 189:476–486
37. Erberich SG, Panigrahy A, Friedlich P, Seri I, Nelson MD, Gilles F (2006) Somatosensory lateralization in the newborn brain. Neuroimage 29:155–161
38. Gilmore JH, Lin W, Prastawa MW et al (2007) Regional gray matter growth, sexual dimorphism, and cerebral asymmetry in the neonatal brain. J Neurosci 27:1255–1260
39. Hüppi PS, Maier SE, Peled S et al (1998) Microstructural development of human newborn cerebral white matter assessed in vivo by diffusion tensor magnetic resonance imaging. Pediatr Res 44:584–590
40. Inder TE, Warfield SK, Wang H, Hüppi PS, Volpe JJ (2005) Abnormal cerebral structure is present at term in premature infants. Pediatrics 115:286–294